Evidence for Electron Density Features That Accompany the Noble Gases Solidification

Roland Boese,* Dieter Bläser, and Oliver Heinemann

Institut für Anorganische Chemie, Universität Essen, 45117 Essen, Germany

Yuri Abramov and Vladimir Tsirelson*

Mendeleev University of Chemical Technology, 125047, Moscow, Russia

Peter Blaha and Karlheinz Schwarz

Institut für Physikalische und Theoretische Chemie, Technische Universität Wien, A-1060 Vienna, Austria

Received: November 17, 1998; In Final Form: May 10, 1999

The structures of krypton and xenon single crystals have been determined by X-ray diffraction at low temperatures. Both noble gases were crystallized by in situ crystallization techniques and found in a face-centered cubic (fcc) type structure. The electron density was reconstructed in both crystals from the X-ray structure amplitudes. It was calculated by full-potential LAPW method at the experimental geometry. A topological electron density analysis and the deformation electron density maps have shown that both Kr and Xe atoms are contracted in the solid state relative to the free atoms and are slightly aspherically polarized to each other, with bridges directed along atom−atom lines. The critical point characteristics indicate the closed-shell interactions in both crystals.

Introduction

All interatomic interactions are classified by description of covalent, ionic, metallic, or van der Waals bonds, which are idealized categories with intermediates in almost all cases we consider. The strong interactions such as covalent or ionic bonds are much better investigated and understood than the weak interactions. However, the latter do not play a less important role in nature. The weakest interatomic forces are the so-called dispersion forces, which are important for the understanding of the solidification of noble gases. Most of the investigations on noble gas solids have been restricted to theoretical considerations,[1] thermodynamical aspects, or the fcc−hcp−bcc phase transitions,[2−4] evidences for which are given by powder diffraction data or thin film deposition.[5] A single-crystal neutron diffraction experiment on fcc xenon at 159.6 K was performed in order to study sound elastic constants.[6] Hitherto, no single-crystal structure X-ray investigations were known for Kr and Xe. Here, we report on the results of an X-ray diffraction investigation of the electron density features of Kr and Xe which accompany the noble gases solidification and present the induction and dispersion force manifestations in noble gas single crystals grown in situ, i.e., directly on the diffractometer.

X-ray diffraction provides the only direct experimental access to the electron density distribution in matter, which governs almost all processes in nature. Unfortunately, the X-ray diffraction experimental data, which were used here in the reconstruction of the electron density features in krypton and xenon single crystals, could not be obtained at the highest possible accuracy level because of intrinsic difficulties arising from the nature of these compounds (see below). Therefore, we have performed the theoretical first-principal calculations for these crystals to put the experimental evidence on a sound theoretical basis.

Experimental Section

Since dispersion forces for noble gases are so small (∼2 kJ mol^{-1}), the melting and boiling points are only 1−4 degrees apart (Kr, mp 116.5, bp 120.9 K; Xe, mp 161.4, bp 165.0 K). This produces experimental problems to grow single crystals from the melt at low temperatures. However, single crystals are the necessary prerequisite to perform X-ray diffraction experiments of solid material in order to gain experimental insight into the electron distribution for the weakest interatomic forces based on electron interactions. For our experiments, we selected krypton and xenon because both can be solidified at liquid nitrogen temperatures. The gases were condensed into thin-walled capillaries attached to a high-vacuum line which were flame-sealed and transferred to a Nicolet R3m/V diffractometer under permanent cooling by flushing with liquid nitrogen with the help of a specially designed device.[7] After several attempts, we succeeded in avoiding the bursting of the capillary. On the diffractometer, the cooling process was taken over by the cold gas stream from a conventional low-temperature device. To grow a single crystal from the polycrystalline solidified material in the capillary, we applied a miniature zone refining procedure by local and careful heating with focused infrared light, a technique that was described before.[8,9] Moving the molten zone along the capillary with simultaneous careful control of the heat source to avoid the boiling of the sample and bursting of the capillary produced a cylindrical crystal. Further experimental problems arose from phase transitions and impurities,[4] as well as from icing of the capillary and geometrical restrictions with the low-temperature device. Various attempts to grow better single crystals, which could be measured at higher diffraction angles, failed, and therefore, the best results for

* Corresponding author. E-mail: boese@structchem.uni-essen.de. Fax: +49-201-183-2535.

10.1021/jp984452y CCC: $18.00
Published on Web 07/16/1999

TABLE 1: Crystal and Conventional Refinement Data

	Kr	Xe
formula weight	83.80	131.30
radiation, λ [Å]	0.7107	0.7107
monochromator	graphite	graphite
temperature [K]	96	145
crystal cylindric, diameter [mm]	0.2	0.3
cell dimension, a [Å]	5.7962(7)	6.3090(7)
cell volume, V [Å^3]	194.73(4)	251.12(5)
no. of reflections for cell determination	31	30
2Θ range for cell determination	20−25	20−25
density, d_{calc} [g m^{-3}]	2.858	3.473
crystal system	cubic	cubic
space group	*Fm*3*m*	*Fm*3*m*
Z	4	4
absorption coefficient, μ [mm^{-1}]	22.60	13.28
$2\Theta_{max}$ for data collection [deg]	60	60
no. measured intensities	535	724
three check reflections, repeated every	50	100
independent intensities	26	34
observed intensities [$I > 2\sigma(I)$]	26	34
no. of reflections for Ψ scans, 10° steps	2	5
R_{merg} before/after correction	0.0332/0.0251	0.0404/0.0367
min/max transmission	0.688/0.755	0.138/0.489
R_{int} (all data, F^2)	0.1551	0.0680
R_σ (all data, F^2)	0.0420	0.0215
R1 [$I > 2\sigma(I)$]	0.0237	0.0416
wR2 (all data)	0.0586	0.1118
GOF (F^2)	1.169	1.150
extinction parameter[a]	0.005(6)	0.011(7)
weighted scheme parameters[a]	0.189/0.0	0.091/0.0
residual electron density [e Å^{-3}]	0.457	1.127
isotropic U value (atom in position 0,0,0)	0.0616(9)	0.0804(13)
parameters refined	3	3
min. atom−atom distance [Å]	4.099(1)	4.461(1)

[a] Parameters as defined in Siemens SHELXTL (ver. 5.03) (1994).

maximum 2Θ angles at 60° are presented only. The determination of cell dimensions and collection of X-ray diffraction intensities as well as a provisional conventional refinement followed standard procedures.[10] These results are given in Table 1. In agreement with early X-ray powder diffraction data[11,12] and neutron diffraction data[6,13] it was found that both Kr and Xe crystallize below their respective melting points in the fcc cubic space group *Fm*3*m*. From the neutron diffraction data, the cell dimensions reported are $a = 5.744(5)$ Å at 77 K for Kr[13] and 6.350(2) Å at 159.6 K for Xe,[6] respectively. Taking into account the high temperature dependence of noble gas solids with the molar volume, our data for Kr and Xe with $a = 5.7962(7)$ and 6.3090(7) Å at 96 and 145 K, respectively, agree with the reported data.

To get information on electronic states of the Kr and Xe atoms in the solid state, the electron densities (ED) of both compounds were then approximated by a flexible κ-model.[14] The ED of each atom in the unit cell was described by the expression $\rho_i = \rho_{core} + P_{val}\kappa^3\rho_{val}$. Here, ρ_{core} and ρ_{val} are the spherically averaged core and valence ED of neutral atoms (the latter are normalized to one electron), κ is a parameter describing the expansion/contraction of atomic electron shells. It is determined together with P_{val}, the electron population of valence shells, by adjustment of the model X-ray structure amplitudes to the experimental ones. This leads to minimal R-factor values when the valence shells of the Kr (Xe) atoms were approximated by 4s and 4p (5s and 5p) functions while $3d^{4d}$ electrons were assigned to the core. The relativistic shell scattering functions[15] were used in the description of ρ_{core} and ρ_{val}. Anomalous scattering corrections were taken from the literature.[16] The thermal motion of atoms was described in the isotropic harmonic approximation. Extinction was taken into account according to ref 17. The isotropic extinction with a Lorentz mosaic block disorientation distribution of 427 and 171 s for Kr and Xe, respectively (the crystal type 1), was observed.

TABLE 2: Results of the Structural κ-model Refinement for Kr and Xe over the Experimental X-Ray Data

	Kr	Xe
R, %	2.18	4.03
R_w, %	2.77	5.62
S	1.07	1.22
w	$1/[\sigma^2 + 0.0001F^2]$	$1/[\sigma^2 + 0.0001F^2]$
U, Å^2	0.0602(3)	0.0800(5)
κ	1.15(7)	1.16(22)
extinction y_{min} for 111 reflection	0.94	0.81

Optimization of the models described (together with the scale factor) was performed with the full data sets by using the MOLDOS96/MOLLY program.[18] The refinement indices and the results obtained are listed in Table 2. Attempts to use the multipole model for the description of the ED of crystals studied failed because of too small sets of the measured structure amplitudes, which were due to the experimental problems described above.

The parameters of the κ-model were used to calculate the model electron density and to find the critical points in both crystals. Critical-point characteristics are given in Table 3. The distributions of the Laplacian of the electron density were calculated as well. Because the Laplacian maps are qualitatively the same, we present here only the map for Kr (Figure 1).

Theoretical

The theoretical calculations were done with the full-potential linearized augmented plane wave (LAPW) method as implemented in the WIEN97 code.[19] A very large basis set (about 600 plane waves) and additional "local orbitals" for the valence s and p states to minimize the linearization error were used. Exchange and correlation were treated with the most advanced version of the generalized gradient approximation (GGA) by Perdew, Burke, and Ernzerhof.[20] The Brillouin zone integration was done with 20 k-points in the irreducible wedge. Theoretical X-ray structure amplitudes up to $\sin\theta/\lambda = 1.4$ Å^{-1} were calculated and the same κ-model was applied to them as was used in the experimental data, thus allowing for consistent comparison between experimental and theoretical results.

An optimized κ-parameter for the sp valence shell of 1.0054 for Kr and 1.0085 for Xe was found, leading to $R = 0.12$ and 0.05% for Kr and Xe, respectively. From the symmetry-allowed multipole terms, the hexadecapole P_{40} appeared to be statistically insignificant, since the refined values of −0.62(72) and −3.07(2.85) for Kr and Xe were about only one esd**.** The critical points in the theoretical model electron density were found (Table 3), and maps of the Laplacian of the electron density were calculated. The latter are very close to the experimental ones and are not presented here.

Because the atomic electron density asphericity is hard to determine with the reciprocal-space model, we calculated the theoretical deformation electron density maps in the position space. They showed a similar pattern for Kr and Xe, hence only the map for Kr is depicted in Figure 2. As can be seen, there is a small contraction of the valence electron density and also a small but significant electron density accumulation along the nearest Kr−Kr distance.

TABLE 3: Critical Point Characteristics for Kr and Xe Crystals (First and Second Rows Represent the Experimental and Theoretical Results, Respectively)

	position of critical point	ρ, e Å^{-3}	λ_1, e Å^{-5}	λ_2, e Å^{-5}	λ_3, e Å^{-5}	$\nabla^2\rho$, e Å^{-5}	type of critical point
Kr	$^1/_4,^1/_4,^1/_2$	0.008(2)	−0.02	−0.02	0.18	0.14(5)	(3,−1)
		0.018	−0.04	−0.04	0.31	0.23	
	$^1/_2,^1/_2,^1/_2$	0.001(1)	0.005	0.005	0.005	0.015(10)	(3,+3)
		0.002	0.01	0.01	0.01	0.03	
	$^1/_3,^1/_3,^2/_3$	0.003(1)	−0.01	0.03	0.03	0.05(2)	(3,+1)
		0.008	−0.01	0.06	0.06	0.11	
Xe	$^1/_4,^1/_4,^1/_2$	0.009(1)	−0.02	−0.02	0.16	0.12(2)	(3,−1)
		0.020	−0.03	−0.03	0.28	0.22	
	$^1/_2,^1/_2,^1/_2$	0.001(1)	0.005	0.005	0.005	0.015(10)	(3,+3)
		0.002	0.01	0.01	0.01	0.03	
	$^1/_3,^1/_3,^2/_3$	0.003(1)	−0.01	0.03	0.03	0.05(2)	(3,+1)
		0.008	−0.01	0.05	0.05	0.09	

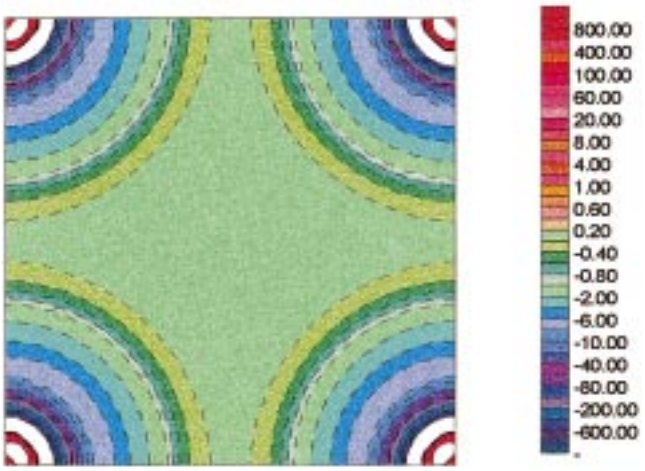

Figure 1. Map of the negative Laplacian of the model electron density, $-\nabla^2\rho$, in the basal plane of the Kr crystal. Contour values are ±0.2, ±0.4, ±0.6, ±0.8, ±1.0 e Å^{-5} increasing in powers of 10 to ±1000 e Å^{-5}. Positive and negative (corresponding to electron deplition) contours are represented by solid and dashed lines, correspondingly. Areas with very large positive and negative values are omitted.

Discussion

The crystal structures of solid krypton and xenon are fcc, and each atom has 12 nearest neighbors. The shortest interatomic distances according to the present study are 4.099(1) Å for krypton and 4.461(1) Å for xenon. The corresponding van der Waals radii, obtained from a supposition of spherical atoms, 2.050 and 2.231 Å, are therefore higher than any ones for Kr and Xe reported previously in the literature.[21,22]

Both electron density and its Laplacian for krypton and xenon crystals are reconstructed from the X-ray diffraction data with limited statistical precision. The density distribution features resulting from the very weak interactions in noble gas crystals studied have significant uncertainty, because of the limited diffraction quality of crystal samples. The accuracy of LAPW calculations is limited as well, and it is very difficult to estimate it qualitatively. It is well-known that all common approximations in density functional theory do not describe van der Waals interactions properly.[23] This was also noted in the present cases. We have found that the theoretical equilibrium volume depends sensitively on the specific approximation used for the description of exchange and correlation effects. It is largely underestimated when using the local density approximation (LDA), but almost by the same amount overestimated when we use the GGA instead. Neither of these two approximations provides a satisfactory description of the theoretical equilibrium volume and thus of the van der Waals bonding in those crystals. We also found some difference in the electron density using these two approximations, where LDA leads, in contrast to GGA, to a more diffuse ED and a much stronger electron density concentration along an atom−atom line, reflecting the well-known overbinding of LDA. In any case, the PBE-GGA is constructed in a way to obey as many known constraints as possible for an exact density functional[20] and is thus, from a theoretical point of view, certainly a better approximation than LDA. Therefore, our analysis is based on the GGA results.

Despite these facts, both experimental and theoretical electron density patterns were the same for both crystals studied. The statistically significant (3,−1) "saddle" critical points are found on the shortest Kr−Kr and Xe−Xe vectors. The positive values of $\nabla^2\rho$ in these critical points (see Table 3) indicate, according to ref 24, the closed-shell interactions in both crystals. Nonempirical quantum chemical calculations[25] have shown that the typical electron density value in (3,−1) critical points in the intermolecular region of the van der Waals molecular complexes is about 0.01 e Å^{-3}. Inspection of Table 3 shows that the value of the theoretical electron density in the (3,−1) critical point on the nearest atom line is also about 0.01 e Å^{-3} in both Kr and Xe crystals. Corresponding experimental electron density values are close to this value as well.

In a very detailed study of the electron density distribution in silicon with excellent diffraction quality,[26] we demonstrated that theoretical and experimental charge densities (or X-ray structure factors) are in rather good agreement with each other, especially when more advanced GGAs[20] are used. The remaining small deviations could be separated into differences in the core and valence charge density. While the core difference is still significant within LDA or most GGA-based calculations (leading to R values of about 0.14−0.20%), the valence charge density agrees quite well using a modern GGA for exchange and correlation. Similar conclusions were reached in the very accurate experimental and theoretical study of urea.[27] That is why we are quite confident that all valence electron density features, resulting from theory, significantly reflect the atomic interactions in the crystals studied. Note that a position−space theoretical calculation (Figure 2) more confidently shows the atomic electron density polarization along atomic interaction lines in the noble gas crystals.

At large distances, mainly dipole−dipole ($\sim R^{-7}$) dispersion forces are responsible for the interaction between the spherical noble gas atoms.[28] This interaction results from electron−electron correlation, a second-order perturbative effect, determined by pair density function in the six-dimensional configurational space of two electrons. As was emphasized recently,[29]

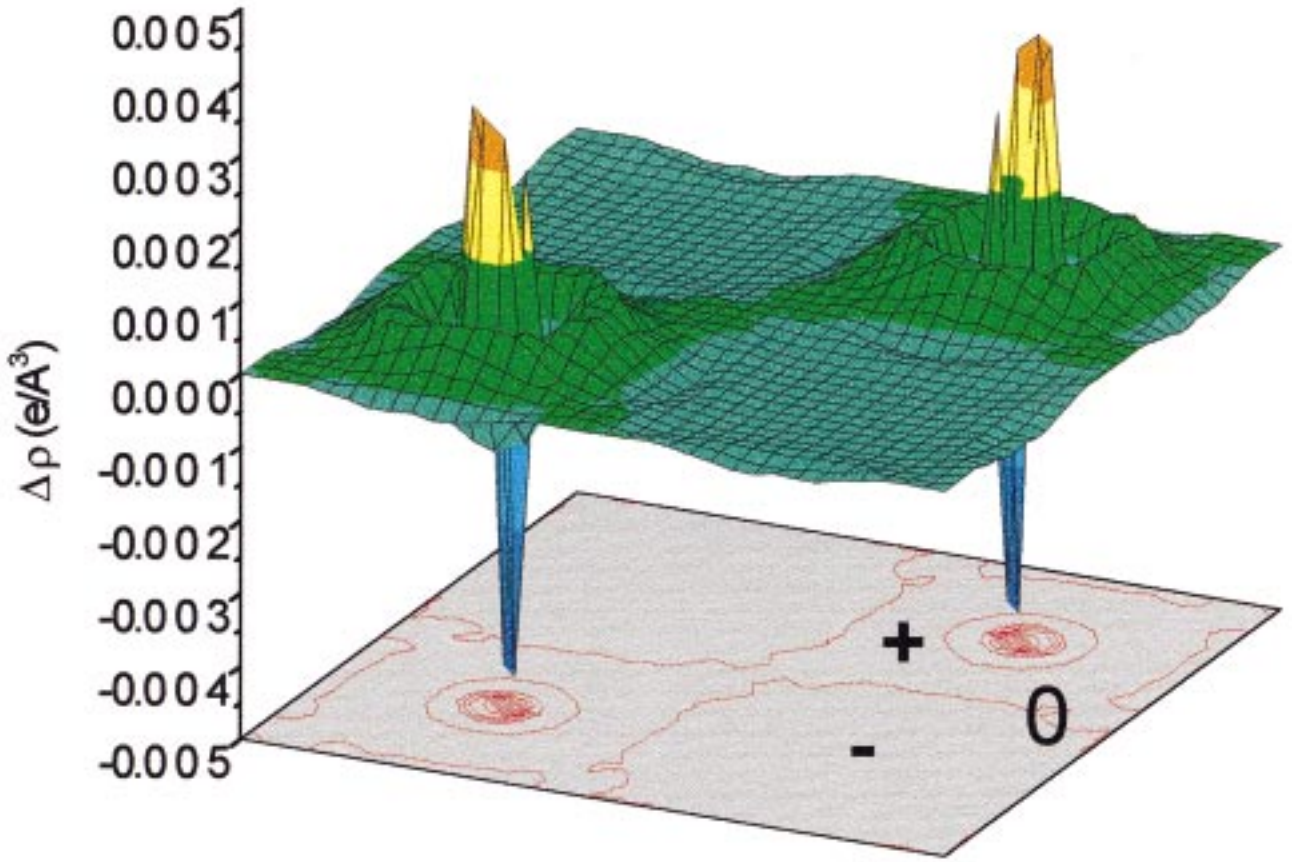

Figure 2. Theoretical deformation electron density map in the basal plane of the Kr crystal.

Feynman[30] found that a net real space manifestation of this interaction is a polarization of the electron density and accumulation of the electrons along atom−atom lines. Corresponding features can be seen in the theoretical deformation electron density map (Figure 2) as small polarization-type bridges directed along lines connecting nearest atoms. Maxima of the electron density concentration on these lines are only about 0.01 e $Å^{-3}$, compared to a value of ∼0.14 e $Å^{-3}$ in the hydrogen bond region of urea.[27] This explains why an attempt to refine the electron occupancies of theses hexadecapole terms was unsuccessful. The LDA approximation led to a slightly more pronounced electron concentration in this region.

The mentioned small hexadecapole-type asphericity of the atomic electron density is only observed in the outer atomic valence electron shells. In general, both Kr and Xe atoms are practically spherical but (judging from the $\kappa > 1$ values) are contracted in the solid state with respect to the free atoms, an effect that is present but much less pronounced in theory. The electrostatic interaction between free atoms is attractive,[31] despite the incomplete screening of the nuclei by the surrounding electron clouds. The contraction of the electron density around the nuclei leads to further reduction of the nuclei−nuclei repulsion due to an additional screening.

The (3,+3) and (3,+1) critical points, corresponding to local minima and two-dimensional minima, respectively, were found at points 1/2,1/2,1/2 and 1/3,1/3,2/3. It is interesting to note that the same pattern of the critical points as in Kr and Xe crystals was found in the study of some fcc metals,[32] which have dramatically different physical properties. The values of the electron density in the critical points are, however, considerably higher in the latter case, which reflects a distinction in the nature of the of the interatomic interaction in these topologically equvalent crystals.

As a conclusion, it should be noted that the X-ray experiments in this study were performed on the limit of the accuracy because of the restricted diffraction quality of the samples of the noble gases studied. At the same time, theoretical calculations using approximations such as LDA or GGA are also on their limit, since the present approximations to the exact DFT functional have restricted accuracy in the proper description of the very weak interactions. However, agreement of the diffraction and theoretical LAPW data allowed us to get a physically and chemically meaningful information about the electron density features in solid Kr and Xe.

Acknowledgment. We gratefully acknowledge Messer-Griesheim for providing the rare gas samples, the Deutsche Forschungsgemeinschaft and the Fonds der Chemischen Industrie for financial help, Professor I. Kaplan and Professor R. F. W Bader for discussion of the results, and Dr. Z. Su for supplying partial relativistic scattering functions. V.G.T. thanks Essen University for Visiting Professorship Award.

References and Notes

(1) Putz, H.; Schoen, J. C.; Jansen, M. *Ber. Bunsen-Ges. Phys. Chem.* **1995**, *99*, 1148.

(2) Klein, M. L.; Venables, J. A. *Rare Gas Solids*; Academic Press: New York, 1976.

(3) hcp, bcc, and fcc structures exists for He, hcp and fcc structures were observed for Ne and Ar; see K. F. Niebel and J. A. Venables in chapter 9 of reference 2. For Kr or Xe, fcc structures are common,[2] and hcp structures were observed in thin films.[4] Phase transitions and twinning occur independent of impurities for Kr and Xe.

(4) Sonnenblick, Y.; Alexander, E.; Kalman, Z. H.; Steinberger, I. T. *Chem. Phys. Lett.* **1977**, *52*, 276.

(5) Gibson, K. D.; Sibener, S. J. *J. Chem. Phys.* **1988**, *88*, 7893.
(6) Lurie, N. A.; Shirane, G.; Skalyo, J., Jr. *Phys. Rev. B* **1974**, *9*, 2661.
(7) Boese, R.; Bläser, D.; Niederprüm, N.; Miebach, T. In *Organic Crystal Chemistry*; Garbarczyk, J.; Jones, D. W., Eds.; IUCr Crystallographic Symposia, Vol. 4; Oxford University Press: Oxford, England, 1991; p 109.
(8) Brodalla, D.; Mootz, D.; Boese, R.; Osswald, W. *J. Appl. Crystallogr.* **1985**, *18*, 316.
(9) Boese, R.; Nussbaumer, M. In *Correlations, Transformations, and Interactions in Organic Crystal Chemistry*; Jones, D. W., Katrusiak, A., Eds.; IUCr Crystallographic Symposia, Vol. 7; Oxford University Press: Oxford, England, 1994; p 20.
(10) (a) *P3/P4-PC-Diffractometer program*, V4.24; Siemens Analytical X-ray Instruments Inc.: Madison, WI, 1989−1991 (for determination of cell dimensions and for data collection). (b) *XDISK Diffractometer data reduction*, version 4.20.2 PC; Siemens Analytical X-ray Instruments Inc.: Madison, WI, 1991 (for data reduction, absorption correction, and correction for cylindrical crystals exceeding the primary beam). (c) *SHELXTL*, version 5.03; a complete package for solving, refining and displaying structures from diffraction data, Siemens Analytical X-ray Instruments Inc.: Madison, WI, 1995.
(11) Barrett, C. S.; Meyer, L. *J. Chem. Phys.* **1964**, *41*, 1078.
(12) Sears, D. R.; Klug, H. P. *J. Chem. Phys.* **1962**, *37*, 3002.
(13) Skalyo, J., Jr.; Endoh, Y.; Shirane, G. *Phys. Rev. B* **1974**, *9*, 1797.
(14) Coppens, P.; Guru Row: T. N.; Leung, P.; Stevens, E. D.; Becker, P.; Yang, Y. W. *Acta Cryst.* **1979**, *A35*, 63.
(15) Su, Z.; Coppens, P. *Acta Cryst.* **1997**, *A53*, 749.
(16) *International Tables for Crystallography*, v. **C**.; Wilson, A. J. C., Ed.; Kluwer Academic Publishers: Dordrecht, 1995.
(17) Becker, P.; Coppens, P. *Acta Cryst.* **1974**, *A30*, 129.
(18) Protas, J. *MOLDOS96/MOLLY IBM PC-DOS*, updated version, 1995 (private communication).
(19) Blaha, P.; Schwarz, K.; Luitz, J. *WIEN97*; Vienna University of Technology: Vienna, 1997 (improved and updated Unix version of the original copyrighted WIEN-code, which was published previously: Blaha, P.; Schwarz, K.; Sorantin, P.; Trickey S. B. *Comput. Phys. Commun.* **1990**, *59*, 339).
(20) Perdew, J. P.; Burke, K.; Ernzerhof, M. *Phys. Rev. Lett.* **1996**, *77*, 3865.
(21) Kihara, T. *Intermolecular Forces*; John Wiley & Sons: Chichester, 1978.
(22) Pyykko, P. *Chem. Rev.* **1997**, *97*, 597.
(23) Perez-Jorda, J. M.; Becke, A. D. *Chem. Phys. Lett.* **1995**, *233*, 134.
(24) Bader, R. F. W. *Atoms in molecules—A Quantum Theory*; International Series of Monographs on Chemistry 22; Oxford University Press: Oxford, 1990.
(25) Bone, R. G. A; Bader, R. F. W. *J. Phys. Chem.* **1996**, *100*, 10892.
(26) Zuo, J. M.; Blaha, P.; Schwarz, K. *J. Phys.: Condens. Matter* **1997**, *9*, 7541.
(27) Zavodnik, V.; Stash, A.; Tsirelson, V.; de Vries, R.; Feil, D. *Acta Cryst.* **1999**, *B55*, 45.
(28) Kaplan., I. G. *Theory of Molecular Interactions*; Amsterdam: Elsevier, 1985.
(29) Bader, R. F. W. *J. Phys. Chem.* **1998**, *102*, 7314.
(30) Feynman, R. *Phys. Rev.* **1939**, *56*, 340.
(31) Hirshfeld, F. L.; Rzotkiewicz, S. *Mol. Phys.* **1974**, *27*, 1319.
(32) Eberhard, M. E.; Donovan, M. M.; Maclaren, J. M.; Clogherty, D. P. *Prog. Surf. Sci.* **1991**, *36*, 1.